

STRUCTURE OF THE GAS DYNAMIC FLOW IN CHANNELS IN THE DETONATION
OF CYLINDRICAL CHARGES OF EXPLOSIVE

V. V. Urban

UDC 533.6

This article examines the formation of a high-speed gas dynamic flow ahead of a detonation wave in a channel. The shock-wave structure of the flow is described and the results of two-dimensional numerical calculations are given.

The gas dynamic flow of detonation products (DP) of cylindrical charges of condensed explosives (EX) having an internal channel or placed inside a large cavity (external channel) is characterized by the formation of shock waves (SW) in the channels. These waves move at a velocity of 10-15 km/sec, which is 1.5-2 times the detonation velocity of the charge. This phenomenon is used in laboratory studies of the acceleration of solid particles [1, 2] and the radiative properties of strong SWs [3, 4] and is of interest in engineering problems. In previous experimental and theoretical studies, investigators have measured the mass velocity of the gas in an internal channel [2, 4, 5], estimated the density of the channel jet [6], qualitatively examined the steady-state pattern of gas dynamic flow [4], and obtained numerical data on the three-dimensional distribution of pressure and velocity [7, 8]. However, as was noted in the survey [9], the structure of the gas dynamic flow in the detonation of cylindrical charges has not been studied in sufficient detail. Here, we describe the shock-wave structure in channels and the region of DP dispersal into the surrounding space in accordance with the results of numerical modeling. We examined changes in the gas dynamic pattern over time and the conditions for the appearance of a high-speed channel flow ahead of the detonation front. This flow is dependent on the dimensions of the channel and the charge.

1. Method of Calculation. We used the approximation of an inviscid gas which does not conduct heat to numerically model the detonation of cylindrical charges of explosive. The dimensions of the channels were chosen to be large enough so that we could ignore the interaction of the shock waves with the boundary layer. The initial system of Euler equations (including the energy source on the detonation front) in a cylindrical coordinate system with axial symmetry was approximated on a finite-difference grid by the Belotserkovskii-Davydov coarse-particle method. This method was substantiated earlier in calculations of two-dimensional nonsteady jets [10, 11]. We used the interpolational equation of state constructed by Kuropatenko [12] to describe the thermodynamic properties of the DPs. In the limiting case of unloading of the DPs to low densities, this equation becomes the equation of an ideal gas with a constant ratio of heat capacities $\gamma \rightarrow 1.375$. The latter is a satisfactory approximation for the description of DPs and air ($\gamma \leq 1.4$) surrounding a charge and filling a channel.

Figure 1a and e, schematize the problem and show the construction of the Eulerian finite-difference grid in the theoretical region ADD'A'. The boundary conditions were assigned as follows: conditions of impermeability on the symmetry axis AA' (Fig. 1a, e) and the walls AD and DD' (Fig. 1e); free outflow on AD and DD' (Fig. 1a). Through calculations were performed. Only in the cells containing undetonated explosive did we use an equation of state with the constant $\gamma = 3$. The width of the region in which the chemical reactions result in the explosive formation of detonation waves (DWs) is on the order of 0.01-0.1 cm [13] for condensed explosives, while satisfactory description of the structure of the detonation front and the gas dynamic flow in a surrounding space of $\sim 100 \times 10$ cm requires a computation grid of approximately $10^4 \times 10^3$ cells (according to [14], ~ 10 cells is needed for the front). To reduce the number of cells in the present investigation, we used a simplified ("discrete")

A. N. Sevchenko Scientific Research Institute of Applied Physical Problems and the V. I. Lenin Belorussian State University, Minsk. Translated from *Inzhenerno-Fizicheskii Zhurnal*, Vol. 57, No. 2, pp. 262-269, August, 1989. Original article submitted February 2, 1988.

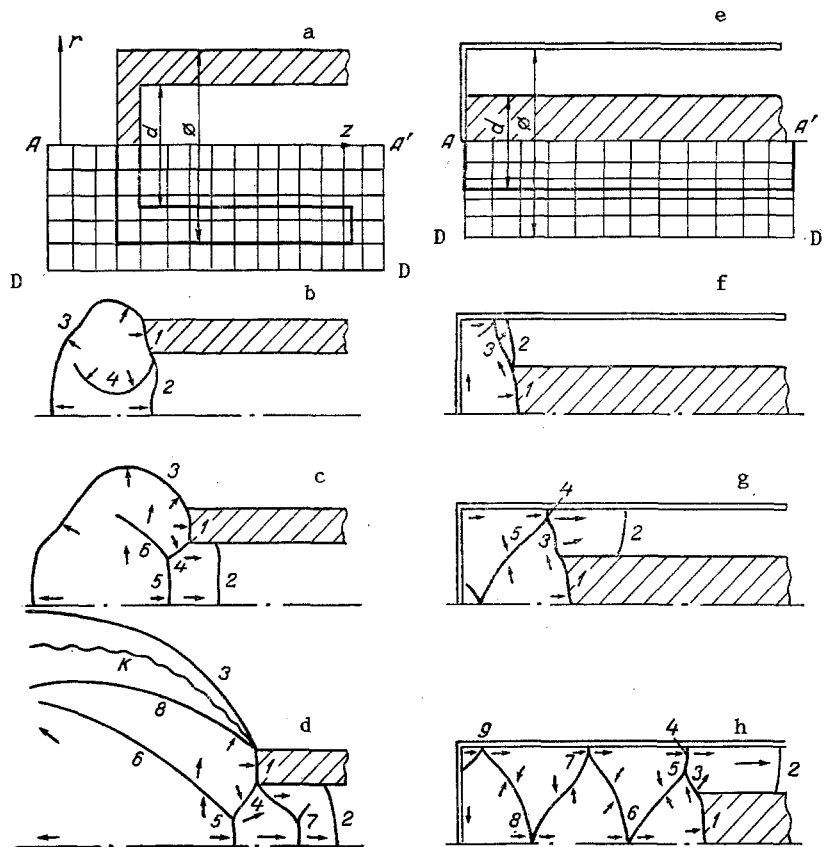


Fig. 1. Construction of finite-difference grid in the theoretical region (a, e) and development of the shock-wave structure for a problem with an internal (b, c, d) and external (f, g, h) channel; the arrows indicate the direction of the mass velocity vector, while the hatched region denotes undetonated explosive.

model of energy release on the detonation front in which the source term Q_j was described as follows:

$$Q_j = Q_v L_j \begin{cases} L_j = 0, & t < z_j/D, \quad t > z_{j+1}/D, \\ L_j = \rho/\rho_j, & t = z_j/D. \end{cases}$$

Energy is released at the moment when the front passes through the j -th cell. After the energy $Q_j \rho_j$ is released in the j -th cell, we calculate the new time of "explosion" of the $j+1$ -st cell $t = z_{j+1}/D$, where $z_{j+1} = z_j + \Delta z$. In the interval $z_j/D < t < z_{j+1}/D$, the DPs may freely flow in the not-yet exploded $j+1$ -st cell. So that the explosion products flowing over into the unreacted cell do not "explode" twice, we chose the source term Q_j in a form that ensures equality of the introduced energy to the energy initially stored in the cold explosive $Q_j \rho_j = Q_v \rho$ for any j . It should be noted that $L_j = 1$ on a Lagrangian grid, where substances are not displaced from one cell to another. If necessary, the detonation process can be calculated more precisely by prescribing the form of the function L_j in the specific kinetic model [15]. Computational features of the model of discrete energy release being used here were studied in test problems. With different conditions of initiation (dynamic loading, thermal heating), we calculated the propagation of a plane SW in the unidimensional case. The resulting profiles of the gas dynamic quantities (pressure, density, velocity, and internal energy) have the same values as would be found with an error of 5-15% on the front of a strong shock wave. In the rarefaction region behind the front, there exists a point $z_g(t)$ which moves at the detonation velocity D - as does the shock wave. The values of all of the gas dynamic quantities at this point coincide with the Chapman-Jouguet values. After the detonation of 20-30 cells, the amplitude of the DW was close to the steady-state value in each variant of initiation in the calculation. In the two-dimensional case with a number of cells ≤ 10 over the radius, rarefaction waves propagating from the lateral surface

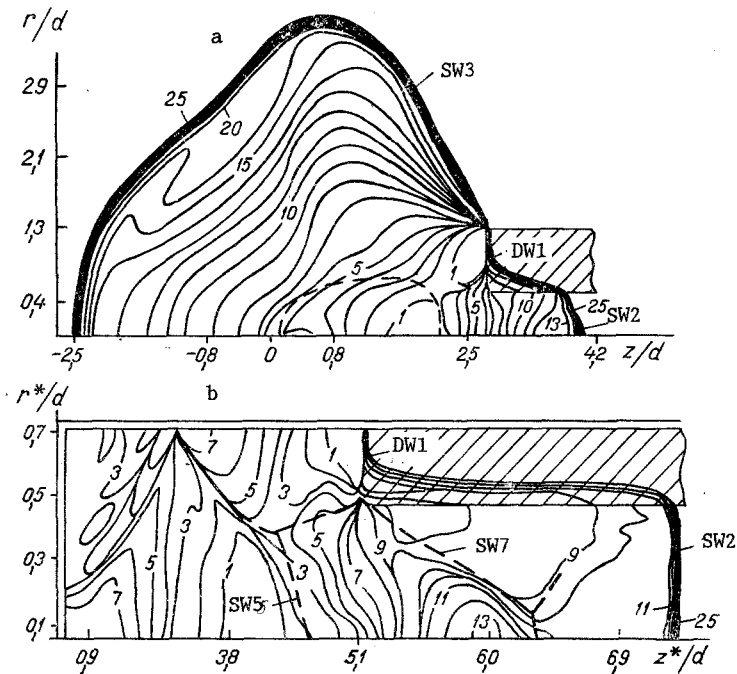


Fig. 2. Three-dimensional flow patterns for two variants of problems with an internal channel at the moments of time 4 μ sec (a) and 26 μ sec (b) (the asterisk denotes that the scale of the coordinates is nonuniform).

of the charge reduce the intensity of the SW to values close to the Chapman-Jouguet values. Since the velocity of the DW and the energy-release balance on the finite-difference grid are satisfied exactly in accordance with the chosen kinetic model, the error of the solution of the problem of the detonation of a charge with dispersal of the DPs in a channel is small. Additional calculations performed with 20-30 cells over the radius showed that for the variants represented in the article, a threefold reduction in pressure at the edge of the charge leads to a 10% reduction in pressure in the Mach wave. Below, we present results of two-dimensional calculations for one type of explosive with the parameters $\rho = 1.6 \text{ g/cm}^3$, $Q_V = 4.5 \text{ kJ/g}$, and $D = 7.3 \text{ km/sec}$. The limiting density and detonation velocity for the explosive in the equation of state [12] were chosen to coincide with explosive TG 50/50.

2. Charge of Explosive with an Internal Channel. Analysis of the literature data and the results of our numerical modeling make it possible to represent the sequence of development of the gas dynamic flow as follows (Fig. 1b, c, d). After explosion of the left end, the front of the DW 1 travels to the bottom of the channel and propagates over the walls of the charge. Unloading of the DPs in the gas filling the channel leads to the formation of the SW 2, which is constricted by the flow from the walls. In the case of a charge without a casing, a SW 3 propagates in the surrounding gas and a compression wave 4 travels toward the symmetry axis of the channel (Fig. 1b). The reflection of the wave 4 from the symmetry axis for different cavity sizes (we examined $d = 1-10 \text{ cm}$) occurs with the formation of a triple shock-wave configuration 4, 5, 6 (Fig. 1c). Here, 5 is the Mach cone, to the left of which is the region of maximum pressure ($\sim 10 \text{ GPa}$) and density ($\sim 1 \text{ g/cm}^3$). The high values of the gas dynamic parameters inside the region of Mach reflection are responsible for the formation of the channel jet. The mach cone 5 of the SW, moving together with the front of the DW, is the "piston" for this jet.

Inside the channel ahead of the DW 1, the gas dynamic flow is rotated so that pressure continuously increases next to the wall of the charge in a "stagnant" zone with a low mass velocity (Fig. 1d). This results in the appearance of a curved discontinuity 7 in the flow, with the transition from supersonic velocity in the flow ahead of the wave 5 to subsonic velocity taking place on this discontinuity. Mach or regular reflections of the discontinuity 7 on the symmetry axis are possible.

If we ignore the change in the velocity and the parameters on the front of the DW due to constriction of the explosive by the pressure of the channel jet and if we assume the detonation parameters to be constant, then the flow pattern for an infinite charge becomes steady. In this case, the jet analogy [16] is valid in the coordinate system of the DW front. In accordance with this analogy in the present case, we can examine the problem of the discharge of a sonic jet from an annular nozzle with a central hole in a co-current supersonic flow. The external part of such a flow is known [16] (Fig. 1d) and consists of an SW 3 (ballistic wave), the contact boundary K, and a suspended shock 8 that develops with stagnation of the expanding supersonic flow of the DP's. Inside the flow, there is a second suspended shock 4 which is irregularly reflected on the symmetry axis (Mach cone). Here, the incoming supersonic flow is slowed, and the SW 2 propagates in the channel. In the region downflow, the discontinuities 6 and 8 may intersect and be repeatedly reflected on the symmetry axis.

Let us examine the results of the numerical calculations. The isobar fields in Fig. 2 were drawn with a logarithmic interval of 0.2 (5 lines per order of magnitude) and have numerical values of 10, 6.39, 3.98, ..., $1.58 \cdot 10^{-4}$ GPa designated by the numbers 1, 2, 3, ..., 25, respectively. The sample results shown in Fig. 2 illustrate the development of the gas dynamic flow for a charge without a casing $d = 1.2$ cm and with a casing $d = 4$ cm at the stage of development of the shockwave structure corresponding to Fig. 1c and d. The positions of DW 1 and SW 2 in the channel and SW 3 in the surrounding gas can be determined from the crowding of the isobars in the high-pressure-gradient region. The curvature of the front of the external SW 3 (Fig. 2a) is due to the nonuniform dispersal of the DPs from the end and lateral surface and is maintained for several tens of ϕ . The scale along the coordinate axes in Fig. 2b ($z > 0$, $r > d$) is nonuniform because the difference grid is constructed with a progressively increasing step size. The constriction of the undetonated explosive by the pressure of the channel flow is visible in the figures, this phenomenon possibly leading to deformation of the detonation front. The position of the Mach configuration of the discontinuities 4, 5, and 6 in the calculations is determined less accurately due to the small pressure gradients in the flow and their blurring by the artificial viscosity of the finite difference method. The approximation position of these discontinuities, shown by the dashed line in Fig. 2, can be determined from analysis of the fields of the vectors of mass velocity, the isolines of density and local sonic velocity, and the Mach numbers. With the detonation of a charge $d = 4$ cm in a nondeformable casing (Fig. 2b), secondary reflections of the discontinuity 6 from the casing and on the symmetry axis are seen in the region of dispersal of the detonation products.

Calculations show that many details of the hydrodynamic pattern change in relation to the value of d , such as the height of the Mach cone, the distance between the cone and the detonation front, and the velocity of the flow in the channel. However, it was established in experiments in [4] that the measured velocity of the SW 2 in the channel remains roughly constant at $d = 0.3$ - 1.5 cm for identical ratios ϕ/d . The presence of such similitude (it exists apparently by virtue of a certain measurement error) can be explained by the fact that the diameter of the Mach cone is nearly equal to the channel diameter in the range $d \leq 2$ cm. In this case, there is no qualitative change in the flow pattern for identical ϕ/d , since the change in pressure in the SW 5 with the reflection of SW 4 on the symmetry axis corresponds to the arrival of the gaseous detonation products due to the simultaneous change in channel diameter d and the thickness of the walls of the charge ($\phi-d$). The Mach disk almost completely covers the channel due to the small gradients of the gas dynamic quantities over the channel radius in different sections (along z) of the jet. Thus, no secondary discontinuities (SW 7) were seen in the channel flow in the calculations or the experiments [4] at the length $z/d \leq 10$ with $d \leq 1.5$ cm. As was noted in [5], such discontinuities are seen only after the DW has traveled a distance corresponding to several tens of z/d .

At $d \geq 3$ cm, the Mach disk becomes significantly smaller than the diameter of the channel, which leads to the earlier appearance of secondary discontinuities SW 7 behind the front of the channel SW 2. Thus, for the computing variant $d = 4$ cm, the creation of an oblique shock 7 is seen at just $z/d = 3.4$ twelve microseconds after the beginning of detonation of the charge. The shock wave 7 is shown at the moment $t = 26$ μ sec by the dashed line in the channel in Fig. 2b.

The change in the flow in the channel with an increase in d can also be seen from a comparison of the profiles of pressure, density, specific energy, and the axial component

of mass velocity on the symmetry axis of the charge in the cases corresponding to Fig. 2. In the case of small $d = 1.2$ cm, the flow structure in the channel changes similarly to the flow in a shock tube [17]. Here, the SW 2 in the "test" gas is joined at the contact boundary with the "pushing" gas flowing from the "reservoir" of SW 5 in the form of a rarefaction wave. At large $d = 4$ cm, the structure is typical of the discharge of an underexpanded jet: There is a decrease in the gas dynamic parameters due to overexpansion of the flow in the supersonic part from the site of SW 5 to the front of SW 7, which separates the supersonic flow from the subsonic flow ahead of SW 2. If we suppose that the role of the "nozzle" in the given case is played by the flow section in the neighborhood of the Mach cone 5, then, in the framework of the jet analogy, the empirically observed [4-6] increase in the velocity of the channel jet with an increase in the thickness of the charge ϕ/d or a decrease in pressure in the channel can be explained by a change in the degree of underexpansion of the jet, i.e., the ratio of pressure on SW 5 to the pressure of the gas in the channel. This is confirmed by calculations of the variants $\phi/d = 1.5-1.7$, in which the velocity of SW 2 increases from 10.2 to 14.3 km/sec on the segment $z/d = 10$.

If we change over to the coordinate system connected with the front of the DW, then in the jet analogy the velocity of SW 2 initially increases during the establishment of the steady-state flow. It then decreases to zero (i.e., to the velocity of the detonation front), obviously due to the finite "range" of the channel jet in the counter-directed supersonic flow. These considerations are consistent with the measurements made at $d = 0.3-1.5$ cm in [5], where the velocities of the SW 2 and DW became the same at the distance $z/d \approx 200-300$.

3. Charge of Explosive Inside a Channel. As far as we know, the problem of the detonation of a cylindrical charge inside a closed cavity has not been studied theoretically. It is easy to see that this reduces to the problem of the detonation of a charge with an internal cavity placed in a deformable casing. Such a deduction becomes obvious if we move the symmetry axis AA' (see Fig. 1e) to the boundary of the theoretical region DD'. Using the same analogy as above, we can describe the following scheme of development of the shock-wave pattern (Fig. 1f, g, h). As the SW 1 propagates through the charge, the explosion products, dispersing in the radial direction, excite SW 2 in the surrounding gas and are reflected from the wall. Their reflection results in the formation of the regular (f) or Mach (g, h) configurations 3, 4, 5. Several successive reflections of the SW from the wall and on the symmetry axis (h) are possible as the flow develops, the number of these reflections depending on the parameters at the detonation front and the dimensions of the channel.

The isobars in Fig. 3 show the theoretical patterns of three-dimensional gas dynamic flow using the example of the variants $\phi/d = 2$ and 3.14 at the moments of time $t = 40$ and 36 μ sec. The numbers next to the lines have the same values as in Fig. 2. The positions of DW 1, SW 2, and reflected SWs 5-9 are determined by the crowding of the isolines at the sites of the largest pressure gradients. Also evident is the compression of the undetonated explosive by the pressure of the channel jet (Fig. 3a). It is evident from a comparison of the theoretical profiles of the main hydrodynamic quantities on the symmetry axis and the channel wall that the flow inside the channel is characterized by lower values of the hydrodynamic parameters behind the Mach cone 4 and in the body of the channel jet than the flow in the internal channel. This difference is due to the fact that the SW is intensified in the internal channel by detonation with convergence on the symmetry axis, while the SW is weakened in the external channel due to divergence of the flow in the expanding volume. Whereas a high-speed jet is formed in the internal channel even with $d = 10$ cm, in the external channel with $d = 3.14$ cm the Mach reflection on the wall is replaced by regular reflection, and there are no jets in advance of the detonation front (Fig. 3b). In this computing variant, the SW undergoes only one reflection from the wall and on the symmetry axis.

The creation of secondary SW 7 behind the front of SW 2 was not observed either in the experiments in [5] or in the completed calculations (Fig. 3a). This can be attributed to weakening of the perturbations propagating radially from the surface of the charge from the low-velocity region in the direction of the channel wall. As a result, no "stagnant" high-pressure zone is formed. We can also expect the flow in the external channel to have one more property. The profiles of the gas dynamic quantities on the channel wall are similar to the flow profiles in a shock tube [7]: located behind the front of SW 2 is a region of nearly constant parameters that connects the rarefaction wave with the Mach disk 4. However, in contrast to a normal SW (behind which the flow is subsonic), the flow here is super-

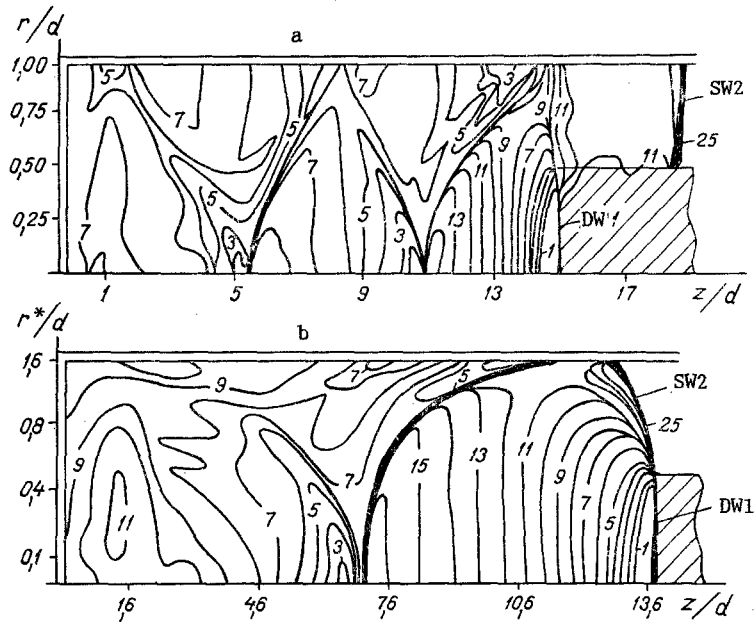


Fig. 3. Three-dimensional flow patterns for two variants of the problem with an external channel at the moments of time 40 μ sec (a) and 36 μ sec (b).

sonic everywhere from SW 4 to SW 2 in the laboratory coordinate system. With a change in $\phi/d = 2-1.35$, the velocity of SW 2 up to $t = 36 \mu\text{sec}$ increases from 9.5 to 12.8 km/sec, while mass velocity changes from 10.3 to 13.7 km/sec. Here, the percentage of kinetic energy in the total energy of the jet changes from 70 to 75%. Thus, the type of flow is typical of shock tubes with an expanding channel [18] and corresponds in our case to a relatively early stage of acceleration of SW 2 in the channel. The coordination of the supersonic flow in the rarefaction wave with the subsonic flow ahead of SW 2 should lead to the appearance of yet another SW in the flow.

The velocities of SW 2 in the internal (D_i) and external (D_0) channels can be compared in terms of the fullness of the channel, having defined the latter as the ratio of its free volume to the volume of explosive: $\beta_i = d_i^2/(\phi^2 - d_i^2)$ and $\beta_0 = (\phi^2 - d_0^2)/d_0^2$. Thus, for $d_i = 1.5$ cm and $d_0 = 1$ cm, we obtain $D_i = D_0 = 10.2$ km/sec with $\beta_i = \beta_0 = 2.6$. If $\beta_i, \beta_0 < 2.6$, then $D_i < D_0$, while at $\beta_i, \beta_0 > 2.6$ we conversely have $D_i > D_0$. It should be noted that this relationship was established at the stage of channel flow during which the velocity of SW 2 increased only slightly and the dimensions of the channel and the Mach disk SW 5 were similar, i.e., in the flow regime characteristic of a shock tube without the appearance of SW 7.

It can be concluded from the above that the most important dimension in the above problem is the diameter of the channel. For any charge thickness there exists a channel diameter such that Mach reflection is replaced by regular reflection and no flow is formed ahead of the detonation front. The gas dynamic flow established in channels with the detonation of cylindrical charges of explosive has a long nonsteady phase characterized by the appearance and interaction of a complex system of SWs and compression waves in the region of DP unloading and in the channel. In this stage, there is a continuous change in the velocity of the front of the channel jet. This velocity reaches a maximum and then, without allowance for wall friction, decreases to the velocity of the DW. For sufficiently large scales of channel flow ($\sim 100 z/d$), conditions may be realized whereby the gas dynamic structure becomes steady. Then, in the coordinate system connected with the detonation front, the structure can be represented as a collection of interacting phenomena occurring in the detonation zone, an underexpanded sonic jet, a co-current supersonic flow, and in a channel jet flowing into a counter-directed supersonic flow.

NOTATION

z, r , axial and radial coordinates; Δz , step of finite-difference grid along the z axis; t , time; D , velocity of the detonation and shock waves; ρ , density of the condensed explosive;

Q_v , specific energy of the explosion at constant volume; d , ϕ , internal and external diameters. Indices: j , index of the cell of the theoretical grid along z ; g , parameters at the Chapman-Jouguet point; i , 0, values of quantities in the internal and external channels.

LITERATURE CITED

1. V. M. Titov, Yu. I. Fadeenko, and N. S. Titova, Dokl. Akad. Nauk SSSR, 180, No. 5, 1051-1052 (1968).
2. V. M. Titov and G. A. Shvetsov, Fiz. Goreniya Vzryva, 6, No. 3, 401-404 (1970).
3. I. F. Zharikov, I. V. Nemchinov, and M. A. Tsikulin, Zh. Prikl. Mekh. Tekh. Fiz., No. 1, 31-44 (1967).
4. M. A. Tsikulin and E. G. Popov, Radiative Properties of Shock Waves in Gases [in Russian], Moscow (1977).
5. A. S. Zagumennov, N. S. Titova, Yu. I. Fadeenko, et al., Zh. Prikl. Mekh. Tekh. Fiz., No. 2, 79-83 (1969).
6. G. V. Pryakhin, V. M. Titov, and G. A. Shvetsov, Zh. Prikl. Mekh. Tekh. Fiz., No. 3, 137-140 (1971).
7. V. F. Lobanov and Yu. I. Fadeenko, Fiz. Goreniya Vzryva, 10, No. 1, 119-124 (1974).
8. V. Z. Kasimov and Yu. P. Khomenko, Problems of Nonsteady Gas Dynamics [in Russian], Tomsk (1984), pp. 62-70.
9. V. B. Mintsev and V. E. Fortov, Teplofiz. Vys. Temp., 20, No. 4, 475-764 (1972).
10. G. S. Romanov and V. V. Urban, Izv. Akad. Nauk SSSR Mekh. Zhidk. Gaza, No. 4, 153-156 (1978).
11. G. S. Romanov and V. V. Urban, Inzh.-Fiz. Zh., 37, No. 5, 859-867 (1979).
12. V. F. Kuropatenko, Chislennye Metody Mekh. Sploshnoi Sredy, 8, No. 6, 68-71 (1977).
13. A. F. Baum, K. P. Stanyukovich, and B. I. Shekhter, Physics of Explosions [in Russian], Moscow (1975).
14. M. V. Batalova, S. M. Bakhrakh, V. L. Zaguskii, et al., Zh. Prikl. Mekh. Tekh. Fiz., No. 3, 73-80 (1971).
15. J. Meider, Numerical Modeling of Detonation [in Russian], Moscow (1985).
16. V. I. Mali, A. K. Rebrov, G. A. Khramov, et al., Fiz. Goreniya Vzryva, 17, No. 3, 122-125 (1981).
17. Ya. B. Zel'dovich and Yu. P. Raizer, Physics of Shock Waves and High-Temperature Hydrodynamic Phenomena [in Russian], Moscow (1963).
18. T. V. Bazhenova and L. G. Gvozdeva, Transient Interactions of Shock Waves [in Russian], Moscow (1977).